

Development of Adaptive Array Antenna for Mobile WiMAX Uplink

Mitsuru HIRAKAWA*, Takashi YAMAMOTO, Yoji OKADA and Mitsuo SUGIMOTO

Mobile Worldwide Interoperability for Microwave Access (Mobile WiMAX) is a next-generation wireless communication technology that enables higher data throughput and better mobility compared to wireless local area network (WLAN). Mobile WiMAX supports a 1-cell reuse pattern for improving spectrum efficiency, but this cell allocation suffers from heavy co-channel interference (CCI). Adaptive array antenna can be an efficient solution for canceling interference signals, but it is difficult to apply a recursive adaptive array algorithm in the multipath environment because uplink user data is distributed over the bandwidth and the channel state changes instantly. To solve this problem, the authors developed a new adaptive array algorithm that calculates adaptive weights to cancel interference signals on a tile-by-tile basis. In their simulation and experiment, the authors verified that demodulation quality is dramatically improved by using the new algorithm instead of the conventional zero-forcing (ZF) algorithm.

1. Introduction

Mobile worldwide interoperability for microwave access (Mobile WiMAX) based on IEEE 802.16e is a standard designed for metropolitan area networks (MAN) that cover an area wider than that covered by local area networks. Commercial WiMAX services are already available in some countries and regions. Services in Japan are scheduled to start in 2009.

Mobile WiMAX supports "one-cell frequency reuse," which allows adjacent cells to use the same frequency. This causes co-channel interference to occur, resulting into degradation of communication quality. It is therefore necessary to cancel interference from other cells to ensure high communication quality. Adaptive array antenna is an effective means of removing interference waves; however, it is difficult to apply the conventional algorithm to the frame configuration in Mobile WiMAX systems.

The authors therefore developed an adaptive array that is optimized for use in Mobile WiMAX uplink. This paper presents the summaries of WiMAX and adaptive array antenna, and describes the algorithm for the newly-developed adaptive array antenna. The results for the simulation tests and experimental tests performed using prototype base stations are also presented at the end of this paper.

2. Mobile WiMAX

Mobile WiMAX is a wireless communications standard for wide-area, high-speed data transmission. It enables wireless broadband access. The following sections describe the frame configuration and access method of Mobile WiMAX.

2-1 Mobile WiMAX Frame Configuration

As shown in Fig. 1, Mobile WiMAX uses the time division duplex (TDD) communication scheme. One frame consists of a downlink (DL) subframe, an uplink (UL)

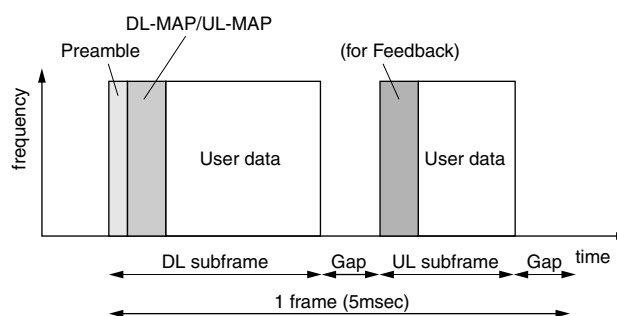


Fig. 1. Mobile WiMAX frame format

subframe, and a gap between the subframes. The DL subframe consists of a preamble used by the mobile station to detect the timing of each frame, a DL-MAP/UL-MAP section that stores the resource allocation information for user data, and user data. The UL subframe consists of a feedback region and user data.

2-2 OFDMA

Mobile WiMAX uses orthogonal frequency division multiple access (OFDMA) for both the uplink and downlink. OFDMA allows multiple users to share the same communication bandwidth so that simultaneous multiple access can be achieved by means of orthogonal frequency division multiplexing (OFDM). The following briefly describes the configuration and operation of an OFDMA transmitter (mobile station) and receiver (base station) in the WiMAX uplink.

Figure 2 shows the configuration of an OFDMA transmitter. The mobile station performs the following operations: (1) Checking UL-MAP information included in the DL subframe, identifying the frequency resource allocated to it, and mapping the transmission data $S_u(m,k)$ to the allocated subcarriers; (2) converting frequency-domain signals $S_u(m,k)$ into time-domain signals $s_u(m,n)$

by means of an inverse fast Fourier transform (IFFT); (3) inserting a cyclic prefix (CP) to improve multipath tolerance; and (4) transmitting signals from the antenna after performing the necessary processing, such as digital-to-analog conversion and frequency conversion. In the above description, m is the OFDM symbol index; k is the subcarrier index; and n is the sample index with a value between 0 and $N-1$ (N : IFFT size).

Figure 3 shows the block diagram of the receiver. The diagram supposes that the tops of the signals from individual mobile stations—that is, the first symbols in the UL subframes—are received at the base station with the same timing. The base station performs the following processes: (1) frequency conversion and analog-to-digital conversion of the received signals; (2) removal of the CP; (3) conversion of the time-domain signals $s'(m,n)$ into frequency-domain signals $S'(m,k)$ by means of a fast Fourier transform (FFT); and (4) channel estimation, signal demodulation, and division of the demodulated signals into U number of user datasets (where U is the number of mobile stations) according to the resource allocation information.

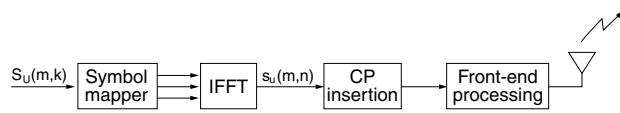


Fig. 2. OFDMA transmitter

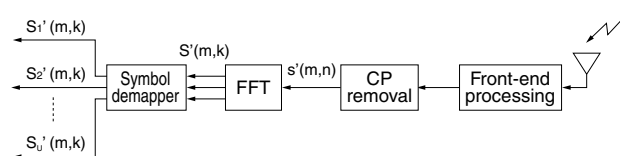


Fig. 3. OFDMA receiver

2-3 Challenges for Mobile WiMAX

Studies are currently underway with Mobile WiMAX to determine whether the same frequency can be used between cells to improve the efficiency of frequency use. If this is done, however, interference from other cells may cause deterioration in the reception quality.

Figure 4 shows the occurrence of interference. Signals from mobile station MS-B2 communicating with the base station in cell B are also received by the base station in cell A in the uplink. Signals from MS-B2 constitute interference for the base station in cell A, and therefore the quality of the uplink signals received from mobile station MS-A1 deteriorates. This is especially obvious at the edge of the cell where the levels of the signals received from MS-B2 and from MS-A1 are similar, causing considerable deterioration. Adaptive array antenna is effective in canceling such interference, because it can remove interference spatially by adaptively adjusting the phases and amplitudes of the signals received by multiple antennas. The following chapter briefly explains adaptive array antenna technology.

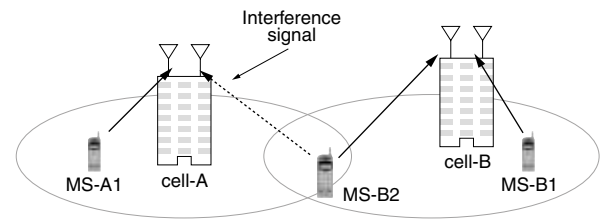


Fig. 4. Interference from another cell

3. Adaptive Array Antennas

The authors made a study on a post-FFT type adaptive array antenna, in which signals are multiplied by weights and combined after FFT. **Figure 5** shows a typical configuration for an adaptive array antenna.

The signals $x_i(m,n)$ (where m is the OFDM symbol index, and n is the OFDM symbol's sample index) received by individual array antennas composed of L number of antenna elements are converted by FFT to frequency domain signals $X_i(m,k)$ (where k is the subcarrier index). The signals of individual subcarriers are multiplied by weights $W_i(k)$ and combined to obtain output signals $Y(m,k)$.

How the weights are calculated in the adaptive array antenna is explained in the following sections. The sections explain two types of adaptive array antenna: one is based on the zero-forcing (ZF) criterion and the other is based on the minimum mean square error (MMSE) criterion.

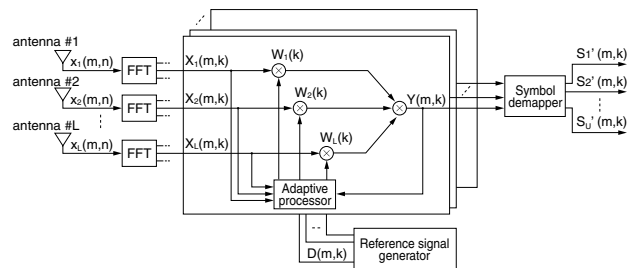


Fig. 5. Adaptive array antenna

3-1 ZF-based Adaptive Array Antenna

The ZF technique forces the channel characteristics to flatten at the receiver end. The procedure is as follows: the channel characteristics $H_i(m,k_p)$ are estimated based on the signals received via the pilot subcarrier k_p onto which the reference signals are mapped, and channel vector $H(m,k_p)$ is configured based on the estimated channel-characteristic values:

$$H(m,k_p) = [H_1(m,k_p) \ H_2(m,k_p) \ \cdots \ H_L(m,k_p)]^T \cdots \cdots \quad (1)$$

where T indicates the transpose. The ZF weight $W_{ZF}(k)$ is obtained from the generalized inverse matrix of $H(m,k_p)$.

$$W_{ZF}^T(m, k_p) = (H^H(m, k_p) H(m, k_p))^{-1} H^H(m, k_p) \cdots \cdots \cdots (2)$$

where H indicates the complex conjugate transpose.

The ZF weight for data subcarriers is normally obtained by interpolating the ZF weight for the pilot subcarriers.

3-2 MMSE-based Adaptive Array Antenna

An MMSE-based adaptive array antenna minimizes error signal, which is equal to the difference between a known reference signal $D(m, k)$ and a combined output signal at the receiving end. Received signal vector $X(m, k)$ and weight vector $W(k)$ for subcarrier k can be expressed as follows:

$$X(m, k) = [X_1(m, k) X_2(m, k) \cdots X_L(m, k)]^T \cdots \cdots \cdots (3)$$

$$W(k) = [W_1(k) W_2(k) \cdots W_L(k)]^T \cdots \cdots \cdots (4)$$

The combined output signal can be obtained from

$$Y(m, k) = \sum_{i=1}^L W_i^*(k) X_i(m, k) = W^H(k) X(m, k) \cdots \cdots \cdots (5)$$

where $*$ indicates the complex conjugate. Based on this equation, the error signal $Err(m, k)$ can be expressed as follows:

$$Err(m, k) = D(m, k) - Y(m, k) = D(m, k) - W^H(k) X(m, k) \cdots (6)$$

The root mean square error is expressed as follows:

$$\begin{aligned} E[|Err(m, k)|^2] &= E[|D(m, k) - W^H(k) X(m, k)|^2] \\ &= E[|D(m, k)|^2] - W^T(k) r_{XD}^*(k) - W^H(k) r_{XD}(k) \\ &\quad + W^H(k) R_{XX}(k) W(k) \cdots \cdots \cdots (7) \end{aligned}$$

where $E[\cdot]$ represents the ensemble average operation. $R_{XX}(k)$ indicating the correlation matrix of the received signals and $r_{XD}(k)$ indicating the correlation vector between the received signals and reference signals are defined as follows:

$$R_{XX}(k) = E[X(m, k) X^H(m, k)] \cdots \cdots \cdots (8)$$

$$r_{XD}(k) = E[X(m, k) D^*(m, k)] \cdots \cdots \cdots (9)$$

The optimal weight $W_{opt}(k)$ that minimizes the root mean square error can be expressed as follows, by making the gradient value $W(k)$ in equation (7) zero:

$$W_{opt}(k) = R_{XX}^{-1}(k) r_{XD}(k) \cdots \cdots \cdots (10)$$

The value thus obtained is called the Wiener solution.

Weight calculation methods can be generally classified as follows: Recursive solution for updating the weight of each symbol (permitted by algorithms such as least mean square (LMS) and recursive least squares (RLS)), and direct solution for calculating the correlation matrix and correlation vector respectively from equations (8) and (9) based on multiple received signals and thus calculating the weights directly using equation (10) (permitted by algorithms such as sample matrix inversion (SMI)).

3-3 Comparison of Weight Calculation Algorithms

Table 1 shows the comparison between different weight calculation algorithms. The ZF algorithm is widely used because it allows instant calculation of the weights

and can also be easily implemented. However, the ZF algorithm does not take into account the influence of interference, and if there is interference, the accuracy of the estimated channel values deteriorates, resulting into significant decrease in the accuracy of weight calculations. In other words, the ZF algorithm is not capable of removing interferences. The authors therefore made a study on the use of MMSE adaptive array antennas with interference removal capability in Mobile WiMAX uplink.

Table 1. Comparison between adaptive array antenna algorithms

	ZF	MMSE		
		LMS	RLS	SMI
Convergence speed	Highly satisfactory	Not satisfactory	Moderately satisfactory	Moderately satisfactory
Interference cancellation	Not satisfactory	Highly satisfactory		
Implementation complexity/ Hardware size	Highly satisfactory	Not satisfactory		

4. Development of Adaptive Array Antenna for Mobile WiMAX Uplink

This chapter describes the problems involved in the use of an MMSE adaptive array for Mobile WiMAX uplink and the algorithm the authors developed to solve those problems.

4-1 Problems in Mobile WiMAX and Development of New Algorithm

Figure 6 shows the UL subframe configuration of Mobile WiMAX. Part of the configuration (circled area in Fig. 6) is enlarged in Fig. 7. Data transmitted from individual mobile stations is stored in the form of tiles, each tile consisting of four pilot subcarriers and eight data subcarriers. The tiles dispersedly exist within the communication band.

Because this frame configuration brings on following problems, the conventional MMSE adaptive array antenna described in Section 3 cannot be used.

- (1) A single UL subframe includes no more than 12 to 18 symbols. For example, Fig. 7 shows that subcarrier 1 (or subcarrier 4) has only four pilot subcarriers for mobile station 1 (MS1) and two pilot subcarriers for mobile station 2 (MS2). Accordingly, a large number of subframes are required for weight convergence, therefore resulting into the considerable degradation of convergence speed.
- (2) Doppler shift and multipath fading change the channel characteristics instantaneously. In addition, interference conditions may change instantly when a mobile station suddenly starts or stops communicating with another base station, or stops communicating with another base station. Such incidents may prevent the weights from converging. In the worst case, the weights may be dispersed.

- (3) Regarding subcarriers 1 to 4 as shown in Fig. 7, because subcarriers 2 and 3 do not include pilot subcarriers, calculation of the weights is not possible. Weight calculation is then performed by interpolating the weights calculated for subcarriers 1 and 4. Before the weight calculation is completed, the data subcarriers' weights cannot be multiplied, and so the data subcarriers need to be stored in memory. For the weights to converge, many subframes are required. With the increase in memory, larger hardware is required, increasing base station size and production costs. Installation becomes more complicated, and processing delays may lower the throughput.

To solve these problems, it is necessary to develop an algorithm that enables fast weight convergence. The authors have developed a new adaptive array antenna that solves these problems. In the newly-developed algorithm, weights are calculated on a tile-by-tile basis, enabling the weights to converge at high speed and the hardware to be small. The new development also has an interference-cancelling function. The following sections discuss the timing/frequency offset correction processes that the authors developed to ensure accurate adaptive array antenna operation, as well as details of the newly-developed adaptive array antenna.

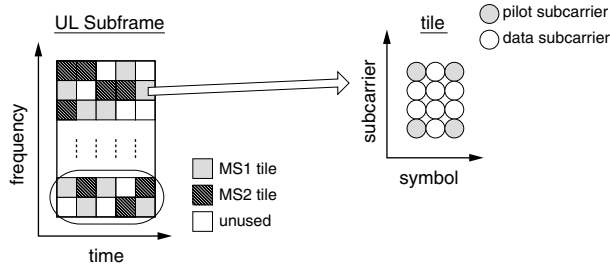


Fig. 6. WiMAX UL subframe and tile

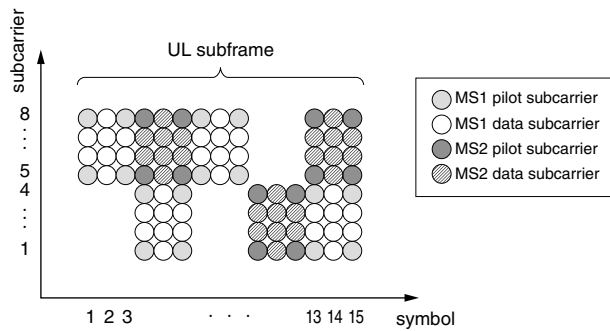


Fig. 7. UL subframe (partial)

4-2 Development of Offset Correction Method

When the carrier frequency of signals transmitted from a mobile station has an offset, the phase of the received signals is rotated because of the influence of the offset. This

phase rotation appears in the time direction. If the timing of signals from a mobile station received by the base station is different from the timing already determined, the phase of the received signals rotates. In this case, the phase rotation appears in the frequency direction. To enable correct operation of the adaptive array antenna, these offsets need to be corrected before weight calculation and combination. This section discusses the offset estimation and offset correction processes the authors developed.

Data transmitted from a mobile station is composed of units called slots, each of which consists of six tiles that align in the frequency direction (24 subcarriers \times 3 symbols). When transmitted from a mobile station, the tiles are dispersed in communication bands. Therefore, in the multipath environment, it is highly probable that each tile received by the base station will have different channel characteristics. However, in the region of 4 subcarriers \times 3 symbols that comprise a tile, the channel characteristics are regarded to be almost the same. Therefore the phase rotation in the frequency direction and symbol direction is influenced extensively by the timing offset and carrier frequency offset. In the new algorithm the authors developed, the phase rotation caused by the offset is calculated for the six dispersed tiles based on the received signal at the pilot subcarrier, and the average of the calculated results is used as the estimated phase rotation. When received signals at pilot subcarriers A, B, C and D at tile t can be defined as shown in Fig. 8, the estimated phase rotation $\hat{\phi}_T$ caused by a timing offset and the estimated phase rotation $\hat{\phi}_F$ caused by a carrier wave frequency offset can be calculated from equations (11) and (12).

$$\hat{\phi}_T = \arg \left\{ \sum_{i=1}^6 [X^{(i)}(m, k)X^{(i)*}(m, k+3) + X^{(i)}(m+2, k)X^{(i)*}(m+2, k+3)] \right\} \cdots \cdots (11)$$

$$\hat{\phi}_F = \arg \left\{ \sum_{i=1}^6 [X^{(i)}(m, k)X^{(i)*}(m+2, k) + X^{(i)}(m, k+3)X^{(i)*}(m+2, k+3)] \right\} \cdots \cdots (12)$$

By correcting the received signals at each subcarrier of six tiles using these estimates, the offset influence can be removed. The adaptive array antenna uses signals whose offsets are corrected.

4-3 Development of Adaptive Array Antenna

When the frequency of the reference signals is different from the frequency required for the weights to converge, the accuracy of weight convergence deteriorates. However, the channel characteristics in a tile are considered to remain almost the same; therefore, the algorithm developed by the authors calculates weights by means of SMI on a tile-by-tile basis.

In Fig. 8, the received-signal vectors at pilot subcarriers A, B, C and D (after offset correction has been performed as in Section 4-2) are expressed as $X_A=X(m, k)$, $X_B=X(m, k+3)$, $X_C=X(m+2, k)$, and $X_D=X(m+2, k+3)$; and the reference signals at pilot subcarriers A, B, C and D are expressed as $D_A=D(m, k)$, $D_B=D(m, k+3)$, $D_C=D(m+2, k)$, $D_D=D(m+2, k+3)$. Based on the explanation given in Section 3-2, the correlation matrix of tile R_{XX_tile} and correlation vector r_{XD_tile} can be calculated from equations (13) and (14), and the optimal weight W_{tile} is calculated from equation (15).

$$R_{XX_tile} = \frac{1}{4} (X_A X_A^H + X_B X_B^H + X_C X_C^H + X_D X_D^H) \dots \dots (13)$$

$$r_{XD_tile} = \frac{1}{4} (X_A D_A^* + X_B D_B^* + X_C D_C^* + X_D D_D^*) \dots \dots (14)$$

$$W_{tile} = R_{XX_tile}^{-1} r_{XD_tile} \dots \dots \dots (15)$$

The combined output signals of data subcarriers 1 to 8 are calculated using the weights obtained from equation (15).

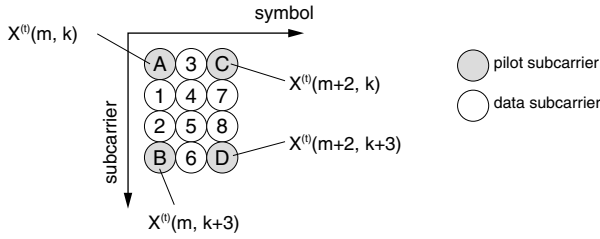


Fig. 8. Tile

5. Numerical Simulation

To confirm the effects of the newly-developed offset correction method and adaptive array antenna, the authors performed a numerical simulation. **Table 2** shows the main parameters of the simulation. One mobile station that attempts communication (desired mobile station) was located in a cell in which the base station was placed, and another mobile station that works as the source of interference (interference mobile station) was located in another cell. The locations of the mobile stations (directions seen from the base station antennas) were determined in a random manner for each slot. The mobile station travel speeds and offset values shown in **Table 2** were also determined randomly for each slot.

Figure 9 shows the cumulative distribution curves of the carrier-to-interference-plus-noise ratio (CINR) of the combined output signals. The horizontal axis represents the CINR values of the combined output signals, and the

Number of BS antennas	2
BS antenna element spacing	4 wavelengths
Modulation method	Quadrature phase shifting keying (QPSK)
MS travel velocity	max. 120km/h
Radio propagation model	Spatial channel model (Urban Macro)
Frequency offset	U (0 – 100 Hz)
Timing offset	N (0, 10 samples)
CNR	30dB
CIR	0dB, 10dB, 20dB
Number of slots subject to evaluation	10,000

vertical axis represents the cumulative probability of being below the CINR. This shows that the newly-developed adaptive-array antenna algorithm is superior to the ZF algorithm. The smaller the carrier-to-interference ratio (CIR), the greater the difference with the ZF algorithm, meaning that the newly-developed algorithm is more advantageous, especially when interference is strong.

Although details are omitted in this paper, in the simulation where no offset correction was performed, the CINR characteristics deteriorated significantly, confirming that the new offset correction algorithm was effective.

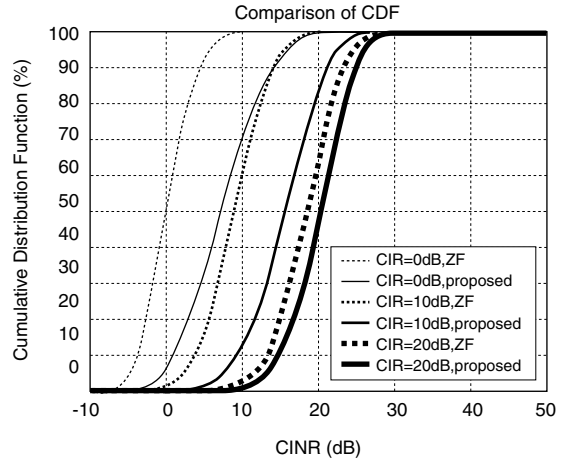


Fig. 9. Comparison of CDF at CINR

6. Experiments Using Prototype

In addition to the simulation described in the previous section, the authors verified their developed adaptive antenna algorithm by installing the new algorithm into a prototype base station DSP. **Figure 10** shows the experimental system. The base station was connected to

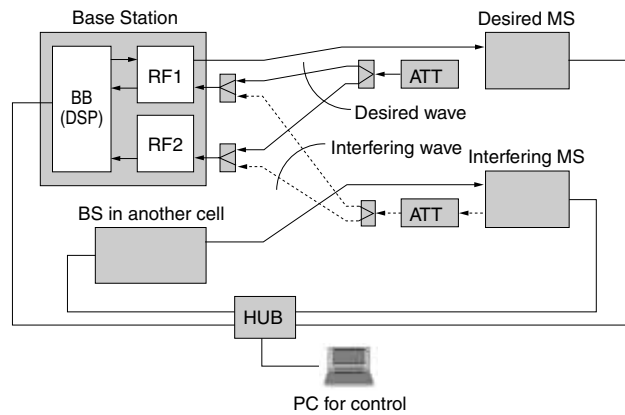


Fig. 10. Test configuration

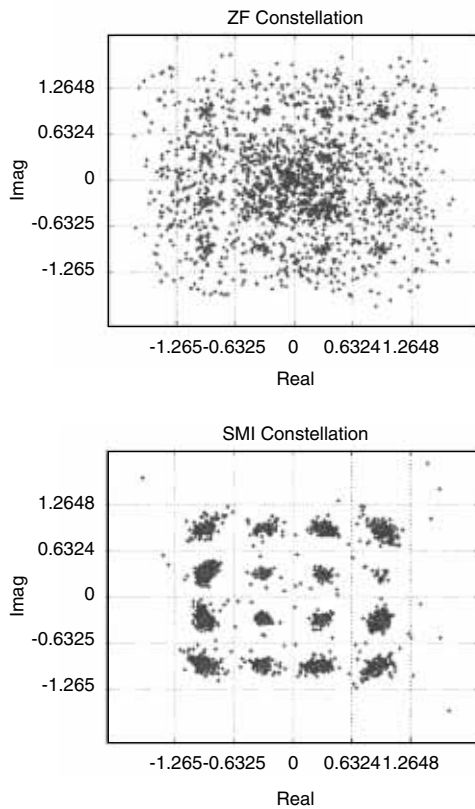


Fig. 11. Received signal constellation (CIR = 0 dB)

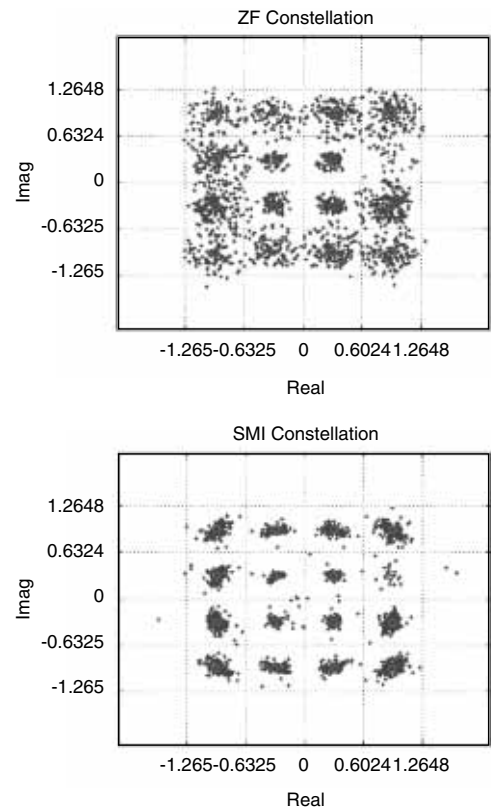


Fig. 12. Received signal constellation (CIR = 10 dB)

a desired mobile station and an interference mobile station via RF cables, and signals from the individual mobile stations were adjusted by an attenuator to obtain the CIR specified for the base station.

Figures 11 and 12 individually show the received signal constellation for CIR = 0 dB and CIR = 10 dB. The modulation method was 16-quadrature amplitude modulation (16QAM). In either case, it was confirmed that the newly-developed adaptive antenna algorithm was superior to the ZF algorithm. Figure 13 shows the results of CINR measurements over a long range of CIR. The figure shows a comparison with the ZF algorithm, shows that in a range where the CIR is small, a maximum CINR gain of 7 dB is obtained. This indicates that the newly-developed algorithm is effective in an interference environment.

7. Conclusions

The authors developed an adaptive array antenna algorithm that enables high-speed weight convergence under interference in the uplink of OFDMA-based Mobile WiMAX, and confirmed that the receiving characteristics are far better than the conventional algorithm by performing simulation and verification experiments using a prototype base station. The adaptive array antenna algorithm developed by the authors is not limited to use in

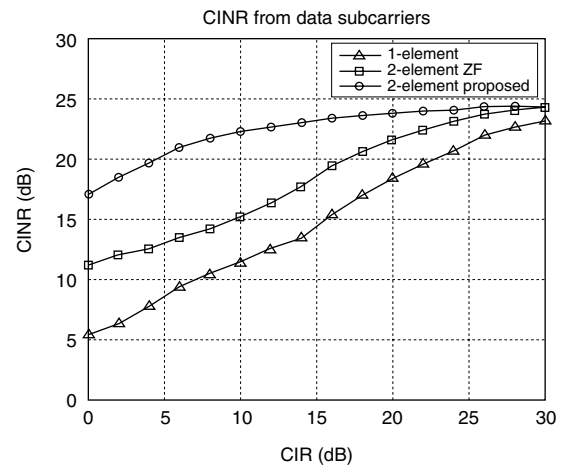


Fig. 13. CINR characteristics at different CIR values

Mobile WiMAX uplink. It can be used in any communications system based on the OFDMA technology.

The authors plan to perform field tests for interference cancellation in future.

References

- (1) IEEE Std 802.16e-2005
- (2) Nobuyoshi Kikuma, "Adaptive Signal Processing with Array Antenna", Science and Technology Publishing Company, Inc., 1999
- (3) 3GPP TS25.996 V6.1.0 (2003-09), "Spatial channel model for Multiple Input Multiple Output (MIMO) simulations (Release 6)"

~~~~~

**Contributors** (The lead author is indicated by an asterisk (\*).)

**M. HIRAKAWA\***

- Senior Research Engineer, Innovation Core SEI, Inc.

He is engaged in the research and development of technologies for processing antenna signals in wireless communications.



**T. YAMAMOTO**

- Transmission System Department, Information & Communication Laboratory

**Y. OKADA**

- Manager, Transmission System Department, Information & Communication Laboratory

**M. SUGIMOTO**

- Senior Assistant Manager, Transmission System Department, Information & Communication Laboratory